〈Research Reports〉 Topographic characteristics of rainfall-induced shallow landslides on granitic hillslopes: A case study in Hofu City, Yamaguchi Prefecture, Japan

Tsukuba Geoenvironmental Sciences, Vol. 13, pp. 23-29, Dec. 22, 2017

Topographic characteristics of rainfall-induced shallow landslides on granitic hillslopes: A case study in Hofu City, Yamaguchi Prefecture, Japan

Kumiko YAMASHITA[a], Tsuyoshi HATTANJI[b], Yasushi TANAKA[c], Shoji DOSHIDA[d] and Takashi MATSUSHIMA[e]

Abstract

Heavy rainfall on July 21, 2009 caused many shallow landslides in Hofu City, western Japan. This paper reports topographic characteristics of shallow landslides in two areas: Yahazugadake area underlain by granodiorite (Gd area) and Tsurugi-kawa area underlain by granite (Gr area). Landslide density (numbers/area) of Gr area was much higher than that of Gd area. For both areas, the landslides had local slopes of 17–46 degrees and specific contributing areas (i.e. drainage area divided by landslide width) of 11–560 m, and there was a weak inverse correlation between local slope and specific catchment area. The landslides in Gd area have steeper local slope and larger specific contributing area than those in Gr area. Field and laboratory measurements of soil properties revealed that the Gr area has thinner soil and higher shear strength for slip plane. Differences in shear strength as well as the hydrological characteristics due to contrasting soil depths are the possible causes of contrasting landslide densities between Gr and Gd areas.

Keywords: high-resolution DEM, hydrological properties, shear strength, slope, soil depth, specific catchment area

1. Introduction

Shallow landslide due to heavy rainfall or strong earthquake is a dominant geomorphic process for slope evolution. Various process-based prediction models of the location of shallow landslides have been developed in recent few decades, where local slope and size of catchment area are major topographic factors for rainfall-induced shallow landslides (Okimura and Ichikawa, 1985; Montgomery and Dietrich, 1989; Dietrich *et al.*, 2001, Uchida *et al.*, 2009). In recent years, development of land survey technologies including air-borne laser scanning enables us to analyze detailed topography of landslide-prone areas using fine resolution (e.g. 1-m grid) DEMs. Such fine-resolution DEMs may improve our understanding of topographic factors for rainfall-induced shallow landslides.

Subsurface structure or lithology also controls susceptibility of rainfall-induced shallow landslides. Many studies conducted detailed field surveys on hillslopes underlain by granitic rocks where shallow landslides were caused by heavy rainfall (Iida and Okunishi, 1983; Okimura, 1983; Ohsaka *et al.*, 1992; Wakatsuki and Matsukura, 2008). Some studies revealed that hillslopes underlain by granite is more susceptible to landslides than those by granodiorite, because of the differences in hydrological properties (Onda, 1992; Wakatsuki and Matsukura, 2008) or shear strength (Terada *et al.*, 1994; Wakatsuki and Matsukura, 2008). However, few studies examined the difference in detailed topographic conditions for shallow landslides between hillslopes underlain by granite and granodiotite.

On 21 July, 2009, heavy rainfall triggered a lot of shallow landslides on granitic hillslopes in Hofu City, Yamaguchi Prefecture, Japan. Although the geological and geomorphological backgrounds have been investigated after this event (Wakatsuki and Ishizawa, 2010; Wakatsuki *et al.*, 2010; Daimaru *et al.*, 2011; Okawa *et al.*, 2012; Matsuzawa *et al.*, 2015), few studies focused on the difference in detailed topographic conditions of shallow landslides between the two areas underlain by granite and granodiorite. We report the contrasting geomorphological features of shallow landslides in granite and granodiorite areas, combining the topographic analysis using 1-m grid DEMs, and field and laboratory measurements of soil properties.

2. Site description

The investigated sites are located in Tsurugi-kawa area and Yahazugatake area in Hofu City, Yamaguchi Prefecture (Fig. 1). Both areas are located at ~5 km north or northeast of the central area of Hofu City, and the elevation ranges from 100 m to 460 m (Figs. 2 and 3). Yahazugatake area (hereafter Gd area) underlain mainly by granodiorite partially with fine-grained bitotite granite, while Tsurugi-kawa

[a] Graduate School of Life and Environmental Sciences, University of Tsukuba, Present: Kokusai Kogyo Co., Ltd.
[b] Faculty of Life and Environmental Sciences, University of Tsukuba
[c] Department of Geography, Faculty of Letters, Komazawa University
[d] National Research Institute of Fire and Disaster
[e] Faculty of Engineering, Information and Systems, University of Tsukuba
Corresponding author: Tsuyoshi Hattanji

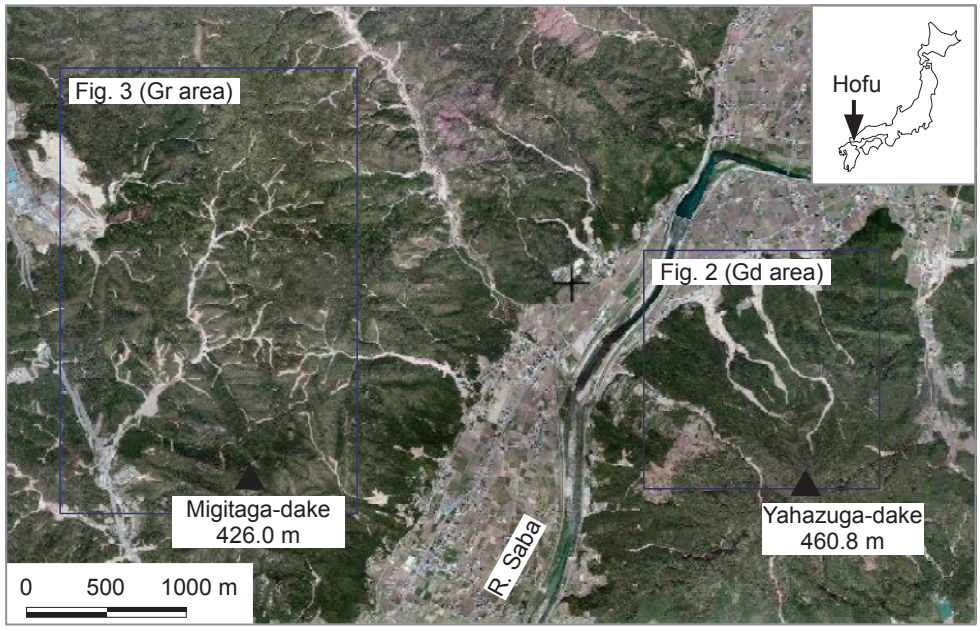

Fig. 1. Aerial photograph of the two investigated areas. Photograph taken in April 2010. Source: Geospatial Information Authority of Japan.

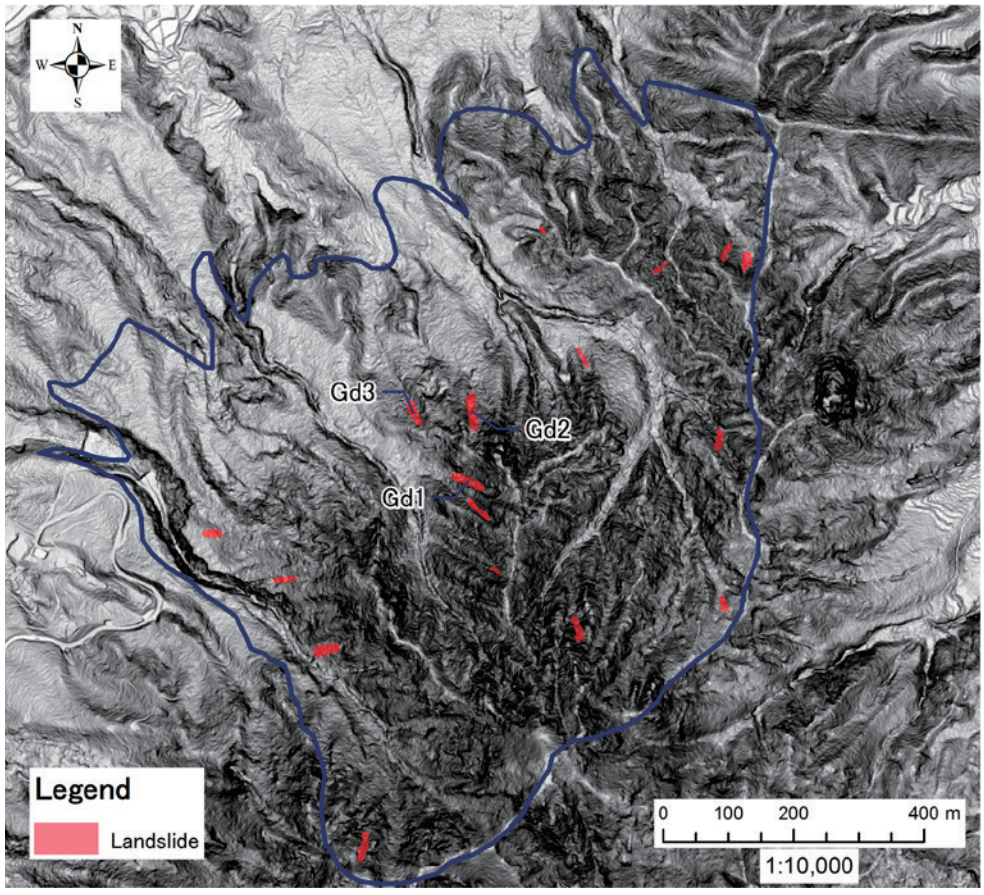

Fig. 2. High-resolution slope map and distribution of shallow landslides in Gd (Yahazugatake) area. The red polygons are landslide sources. Source: Yamaguchi Office of River and National Highway in Chugoku Regional Development Bureau, MLIT.

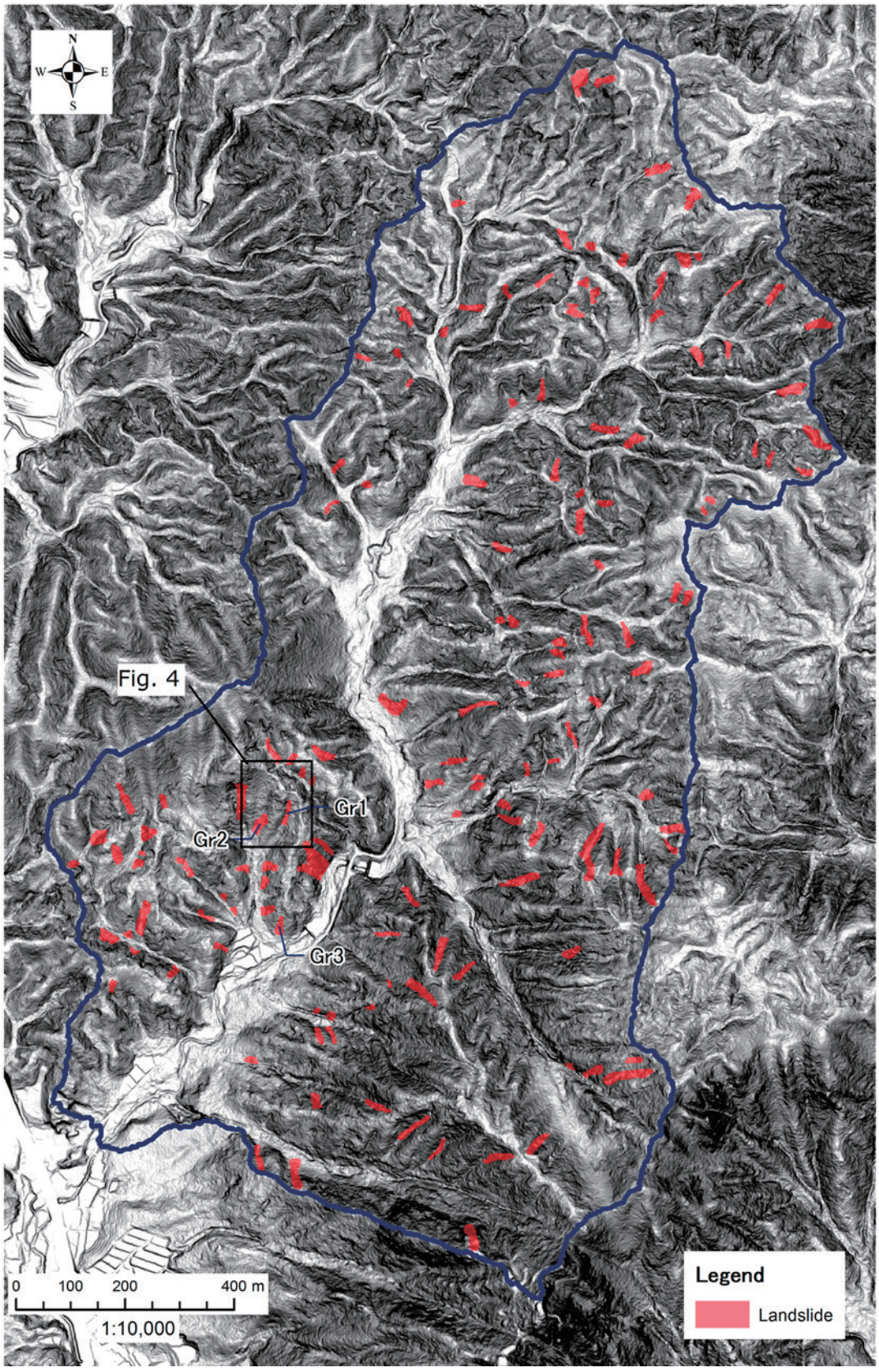

Fig. 3. High-resolution slope map and distribution of shallow landslides in Gr (Tsurugi-kawa) area. The red polygons are landslide sources. Source: Yamaguchi Office of River and National Highway in Chugoku Regional Development Bureau, MLIT.

area (hereafter, Gr area) is underlain by biotite granite with dikes of quartz porphyry (Okawa *et al.*, 2012). Vegetation of these areas is mainly Japanese red pine. In addition, ferns densely cover the ground surface in some parts of the investigated areas. The poor vegetation and sparse exposures of core stones are originated from forest cutting since 17th century (Daimaru *et al.*, 2011).

3. Methods

3.1. Field and laboratory measurements of soil properties

We examined detailed topography, lithology and subsurface structure of three shallow landslides in Gd area (sites Gd1 – Gd3) and three in Gr area (sites Gr1 – Gr3). Cone penetration tests were conducted at top, right-side, and left-side scarps for sites Gd1, Gd3, Gr1, and Gr3. The penetration resistance is represented with *Nc* value, which is the number of impacts required for a penetration of 10 cm (Wakatsuki and Matsukura, 2008). Direct *in situ* shear test with a vane shear tester was conducted at sites Gd3 and Gr3. The vane shear tester is composed of a proving ring for normal stress at the top, a torque meter for shearing stress, a handle for rotating, and a cylinder with eight rectangular vanes at the base. The details of the tester were written in Matsukura and Tanaka (1983) and Wakatsuki *et al.* (2005). The cylinder with vanes was shallowly embedded in the slip plane, and then rotated slowly under the normal stresses of 5.7, 13.8, 22.7 and 31.6 kPa. We both measured shear strength at unsaturated condition with natural soil water contents and saturated condition, in which water is supplied before and throughout the test. Soil samples were taken from sites Gd1, Gd3, Gr1, and Gr3 to measure saturated hydraulic conductivity, particle density and dry bulk density.

3.2. Topographic analysis

Topographic analysis of shallow landslides was conducted with ArcGIS 10.0 (ESRI) and 1-m grid DEMs before (2005) and after the landslide event (2009). These DEMs were offered from Yamaguchi Office of River and National Highway in Chugoku Regional Development Bureau, MLIT. Landslide sources (area of red polygons in Fig. 4) in the event of 2009 were detected from the surface lowering more than 1 m between DEMs in 2005 and those in 2009.

Length of landslide source was measured along a longitudinal line from foot to head scarp. Slope of landslide source, S (= tanθ), was calculated with relative height and horizontal length of the longitudinal line. Width of landslide source, b, was measured along a cross section, which is perpendicular to the longitudinal line at an upslope section of the landslide source.

Size of upslope contributing area area of the green polygons in Fig. 4 for landslide source was calculated with the D-infinity flow method. The calculation procedure is based on Tarboton (1997) as follows; "*The procedure is based on representing flow direction as a single angle taken as the steepest downward slope on the eight triangular facets centered at each grid point. Upslope area is then calculated by proportioning flow between two downslope pixels according to how close this flow direction is to the direct angle to the downslope pixel*". Here we defined the contributing area of landslide source, A, as the sum of the drainage areas of the cells along the cross section used for the calculation of landslide width, b. Specific contributing area, a (= A/b), for each landslide is contributing area divided by width of the landslide (Fig. 4). The program proposed by Perron (2013) was used for the calculation of contributing area.

4. Results

4.1. Field and laboratory measurements of soil properties

Table 1 shows the topographic characteristics of the investigated landslides. The landslides in Gd area have depths of 0.6–2.8 m and slope angles of 34–36°. The landslides in Gr area were shallower (0.5–1.7 m) and gentler (29–33°). Both areas have similar dry bulk densities (mean: 1.28 g/cm³ for Gd1/Gd3, and 1.26 g/cm³ for Gr1/Gr3). Logarithmic mean of saturated hydraulic conductivity in Gd1 and Gd3 (1.8×10^{-2} cm/s, n = 10) were larger than that in Gr1 and Gr3 (5.6×10^{-3} cm/s, n = 10). Particle densities of soil at two sites (Gd1 and Gr1) were

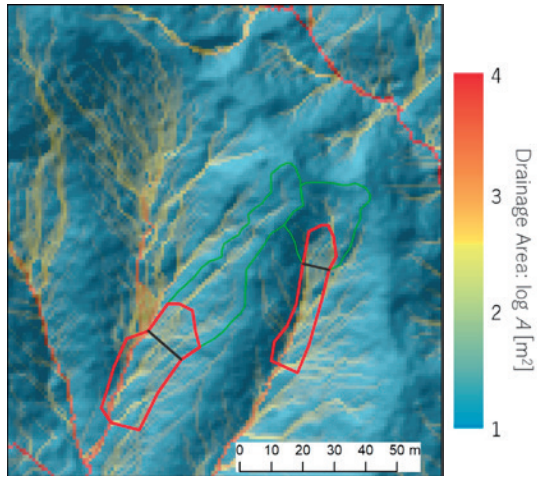

Fig. 4. Measurement of contributing area, A, and landslide width, b, at Gr1 and Gr2. The red polygons are landslide sources, and the green polygons are upslope contributing areas for the landslides at a cross section (black line). Drainage area of each pixel was calculated with D-infinity method, and A is the cumulative value of each pixel that intersects the black line.

Table 1 Dimensions and soil depths of the investigated landslides

site	dimensions of landslide source				soil depth
	width (m)	length (m)	depth (m)	slope (°)	(m)
Gd1	8	25	1.2 – 1.9	35.6	1.3 – 2.3
Gd2	11	35	1.9 – 2.8	35.8	n.a.
Gd3	5	15	0.6 – 1.1	34.7	2.4 – 3.7
Gr1	6	20	0.5 – 1.5	30.4	1.1 – 1.4
Gr2	11	20	1.4 – 1.7	29.4	n.a.
Gr3	7	20	0.9 – 1.2	33.3	0.8 – 1.5

almost same (2.66 g/cm³ for Gd1; 2.67 g/cm³ for Gr1). Cone penetration test clearly indicates that soil-bedrock boundaries (*Nc* = 30) in Gd area (> 2 m) were deeper than those in Gr area (< 1.5 m, Fig. 5). The boundaries of loose and dense soil layers (*Nc* = 5) in Gd area (0.8–1.7 m) were also deeper than those in Gr area (0.5–1.2 m). Table 2 shows the results of direct *in situ* shear tests on a slip plane of Gd3 and Gr3 sites. Although strength data of both sites were similar for natural condition, Gd3 site has larger cohesion than Gr3 site under saturated condition.

4.2. Topographic analysis

Total 145 landslides were detected in Gr area. The number of landslides in Gd area was only 17, and the landslide density of Gd area (20.8 km^{-2}) was significantly smaller than that of Gr area (78.9 km^{-2}).

Fig. 6 plotted specific contributing area, *a*, against local slope, *S* for 137 landslides in Gr area and 17 landslides in Gd area. We excluded eight landslides in Gr area that were probably triggered by bank erosion of debris flows along the main streams. Slopes ranged from 17–47°

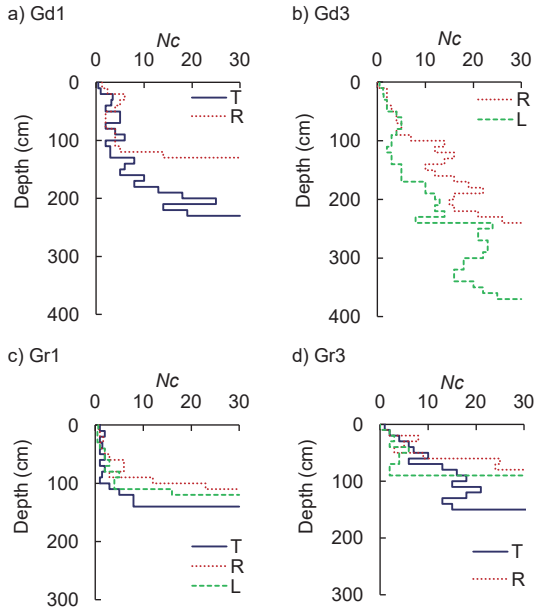

Fig. 5. Depth profiles of *Nc* values of cone penetration tests at landslides Gd1 (a), Gd3 (b), Gr1 (c) and Gr3 (d). The investigation sites are located immediately above top scarp (abbreviated to T), right-side scarp (R) and left-side scarp (L) of the landslide source.

Table 2 Shear strength parameters of slip plane at Gd3 and Gr3 sites

site	φ nat. (°)	c nat. (kPa)	φ sat. (°)	c sat. (kPa)
Gd3	46.7	8.31	44.5	4.55
Gr3	42.9	10.4	47.1	0.28

φ: angle of shearing resistance; c: cohesion
nat.: condition of natural water content;
sat.: saturated condition.

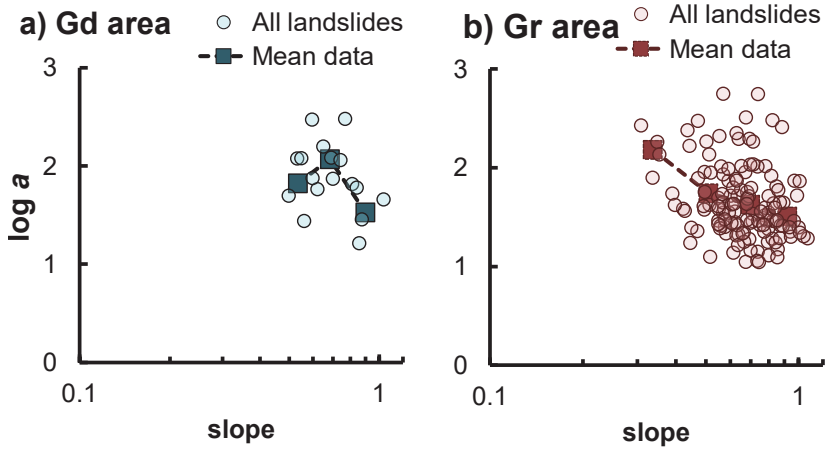

Fig. 6. Specific contributing area plotted against local slope (tangent) of shallow landslides in Hofu City. a) Gr area, and b) Gd area. Unit of *a* value is meter. Plots of mean data refer mean slope and mean *a* values for each slope class (10–20°, 20–30°, 30–40° and 40–50°).

(mean: 33.6°), and *a* values ranged from 11 to 560 m (logarithmic mean: 45 m) for Gr area. Although the plots for all landslides were scattered, mean *a* values for four slope classes (10–20°, 20–30°, 30–40° and 40–50°) showed an inverse trend, which is a decrease of *a* values with increasing slope. Landslides in Gd area have slightly larger *a* values (log. mean: 76 m) than those in Gr area, while slope (mean: 34.7°) is almost same. The slope class of 30–40° for Gd area had significantly higher *a* values (log. mean: 117 m) than that for Gr area (log. mean: 42 m).

5. Discussion

Landslide density of Gr area was significantly larger than that of Gd area. The contrasting landslide densities are related to the difference in specific contributing area for the same slope conditions, in other words, shallow landslides of Gr area occurred with smaller specific contributing area than those of Gd area. The difference of specific contributing area between the two areas was prominent at the slope class of 30–40°. The possible causes for the contrasting landslide responses to rainfall between two areas are the differences in (1) shear strength and (2) pore water pressure during storm. Although the number of measurement was limited, larger soil cohesion must contribute to higher slope stability in Gd area. Two case studies in Abukuma Mountains also reported high shear strength for slopes underlain by granodiorite (Terada *et al.*, 1994; Wakatsuki and Matsukura, 2008). In addition, thinner soil and smaller saturated hydraulic conductivity may facilitate the saturation of soil during storm in Gr area, and causes higher pore water pressure on slip plane (Onda, 1992; Wakatsuki and Matsukura, 2008). Higher pore water pressure due to thinner soil may also reduce slope stability during storms in Gr area.

Although the present paper focused on the difference between Gr and Gd areas in Hofu City, the number of analyzed landslides was still not enough, particularly in Gd area. Further analysis is required for discussion on the contrasting landslide densities between Gr and Gd areas.

Acknowledgements

This study has been financially supported by MLIT Construction Technology Research and Development Subsidy Program (No.91), Fukutake Science and Culture Foundation (11-022) and JSPS Grants-in-Aid for Scientific Research C (16K01214). We thank to Yamaguchi Office of River and National Highway in Chugoku Regional Development Bureau, MLIT for supplying original data of DEMs, to all faculties in geomorphology group of University of Tsukuba and Dr. Wakatsuki, T. (NIED) for valuable comments and discussion, and also to Akiyama, S., Aoki, S., Hoang G. Q., Numata, S., Takahashi, D., Takeda, N., and Yanagiba, S. for assisting field work.

References

Daimaru, H., Tada, Y., Murakami, W. and Ogawa, Y. (2011): Landslides occurred around Houfu City, Yamaguchi Prefecture in 2009: Historical backgrounds. *Journal of the Japan Society of Erosion Control Engineering*, **64** (4), 52–55. (in Japanese)

Dietrich, W.E., Bellugi, D. and Real de Asua, R. (2001): Validation of the shallow landslide model, SHALSTAB, for forest management. In Wigmosta, M.S. and Burges, S.J., eds., *Land Use and Watersheds: Human Influence on Hydrology and Geomorphology in Urban and Forest Areas*, AGU, Washington, D.C., 195–227.

Iida, T. and Okunishi, K. (1983): Development of hillslope due to landslides. *Zeitschrift für Geomorphologie N.F., Supplement band*, **46**, 67–77.

Matsukura, Y. and Tanaka, Y. (1983): Stability analysis for soil slips of two Gruss-slopes in southern Abukuma Mountains, Japan. *Transactions, Japanese Geomorphological Union*, **4**, 229– 239.

Matsuzawa, M., Kinoshita, A., Takahara, T. and Ishizuka, T. (2015): The effects of the degree of mountain denudation on soil layer structure, shallow landslide properties on granite area in Japan. *Transactions, Japanese Geomorphological Union*, **36**, 23–48. (in Japanese with English abstract)

Montgomery, D.R. and Dietrich, W.E. (1989): Source areas, drainage density, and channel initiation. *Water Resources Research*, **25**, 1907–1918.

Ohsaka, O., Tamura, T., Kubota, J. and Tsukamoto, Y. (1992): Process study of the soil stratification on weathered granite slopes. *Journal of the Japan Society of Erosion Control Engineering*, **45** (3), 3–12. (in Japanese with English abstract)

Okimura, T. (1983): A slope stability method for predicting rapid mass movements on granite slopes. *Natural Disaster Science*, **5**, 13–30.

Okimura, T. and Ichikawa, R. (1985): A prediction method for surface failures by mass movements of infiltrated water in a surface soil layer. *Natural Disaster Science*, **7**, 41–51.

Onda, Y. (1992): Influence of water storage capacity in the regolith zone on hydrological characteristics, slope processes, and slope form. *Zeitschrift für Geomorphologie N.F.*, **36**, 165–178.

Okawa, Y., Kanaori, Y. and Imaoka, T. (2012): Distribution and characteristics of debris flows occurred in the Cretaceous Hofu Granitic Region, Yamaguchi

Prefecture. *Journal of the Japan Society of Engineering Geology*, **52**, 248–255. (in Japanese with English abstract)

Perron, J.T. (2013): TopoTools: Analysis of gridded elevation data in Matlab (Version 1.3). http://web.mit.edu/perron/www/downloads.html

Tarboton, D.G. (1997): A new method for the determination of flow directions and contributing areas in grid digital elevation models. *Water Resources Research*, **33**, 309–319.

Terada, K., Hirose, T. and Matsukura, Y. (1994): Measurement of soil properties and slope instability analysis in four small catchments with different bedrock types in the Abukuma Mountains. *Bulletin of the Environmental Research Center, University of Tsukuba*, **19**, 19–31. (in Japanese)

Uchida, T., Mori, N., Tamura, K., Terada, H., Takiguchi, S. and Kamee, K. (2009): The role of data preparation on shallow landslide prediction. *Journal of the Japan Society of Erosion Control Engineering*, **62** (1), 23–31. (in Japanese with English abstract)

Wakatsuki, T., Tanaka, Y. and Matsukura, Y. (2005): Soil slips on weathering-limited slopes underlain by coarse-grained granite or fine-grained gneiss near Seoul, Republic of Korea. *Catena*, **60**, 181–203.

Wakatsuki, T. and Matsukura, Y. (2008): Lithological effects in soil formation and soil slips on weathering-limited slopes underlain by granitic bedrocks in Japan. *Catena*, **72**, 153–168.

Wakatsuki, T. and Ishizawa, T. (2010): Geomorphological characteristics of debris-flow basins in granitic mountain: A case study on a disaster caused by heavy rainfall on July 2009 in Hofu and Yamaguchi Cities, Japan. *Transactions, Japanese Geomorphological Union*, **31**, 423–436. (in Japanese with English abstract)

Wakatsuki, T., Ishizawa, T., Uetake, M. and Kawada, S. (2010): Characteristics of debris flow and slope failure on granite slopes caused by heavy rainfall on July 2009 in Hofu and Yamaguchi Cities, Japan. *Natural Disaster Research Report of NIED*, **44**, 39–51. (in Japanese with English abstract)

Received 8 September, 2017
Accepted 1 November, 2017